doi:10.1016/j.jmb.2010.12.039 J. Mol. Biol. (2011) 406, 503–515

Contents lists available at www.sciencedirect.com

Journal of Molecular Biology

journal homepage: http://ees.elsevier.com.jmb

Two Endoplasmic Reticulum PDI Peroxidases Increase the Efficiency of the Use of Peroxide during Disulfide Bond Formation

Van Dat Nguyen[1], Mirva J. Saaranen[1], Anna-Riikka Karala[1], Anna-Kaisa Lappi[1], Lei Wang[2], Irina B. Raykhel[1], Heli I. Alanen[1], Kirsi E. H. Salo[1], Chih-chen Wang[2] and Lloyd W. Ruddock[1]*

[1]*Department of Biochemistry, University of Oulu, Linnanmaa Campus, 90570 Oulu, Finland*
[2]*National Laboratory of Biomacromolecules, Institute of Biophysics, Chinese Academy of Sciences, Beijing 100101, China*

Received 4 November 2010; received in revised form 23 December 2010; accepted 28 December 2010
Available online 5 January 2011

Edited by F. Schmid

Keywords:
oxidative protein folding; protein disulfide isomerase; hydrogen peroxide; glutathione peroxidase; thioredoxin fold

Disulfide bond formation in the endoplasmic reticulum by the sulfhydryl oxidase Ero1 family is thought to be accompanied by the concomitant formation of hydrogen peroxide. Since secretory cells can make substantial amounts of proteins that contain disulfide bonds, the production of this reactive oxygen species could have potentially lethal consequences. Here, we show that two human proteins, GPx7 and GPx8, labeled as secreted glutathione peroxidases, are actually endoplasmic reticulum-resident protein disulfide isomerase peroxidases. *In vitro*, the addition of GPx7 or GPx8 to a folding protein along with protein disulfide isomerase and peroxide enables the efficient oxidative refolding of a reduced denatured protein. Furthermore, both GPx7 and GPx8 interact with Ero1α *in vivo*, and GPx7 significantly increases oxygen consumption by Ero1α *in vitro*. Hence, GPx7 and GPx8 may represent a novel route for the productive use of peroxide produced by Ero1α during disulfide bond formation.

© 2011 Elsevier Ltd. All rights reserved.

Introduction

Disulfide bond formation in the endoplasmic reticulum (ER) is a redox-dependent process. In addition to the oxidation of dithiols in folding proteins to the disulfide state, *in vitro* one of the key components of the system, Ero1, generates hydrogen peroxide as a "by-product."[1–3] The production of such a reactive oxygen species (ROS) in large amounts is potentially detrimental to the cell. Considerable attention has focused on this, particularly the determination of the elaborate regulatory mechanisms of human Ero1α.[4,5] However, regulation of Ero1α activity is essential to maintaining the optimal redox environment for oxidative protein folding, which requires not only oxidation but also isomerization and reduction of incorrect disulfide bonds to reach the native state. Hence, regulation of Ero1α does not necessarily imply that this has arisen to minimize ROS production, although it does potentially prevent excess ROS production through futile cycling. There is also the potential for one molecule of molecular oxygen to be the electron acceptor for the formation of two disulfide bonds

**Corresponding author*. E-mail address: lloyd.ruddock@oulu.fi.

Abbreviations used: ER, endoplasmic reticulum; ROS, reactive oxygen species; PDI, protein disulfide isomerase; GPx, glutathione peroxidase; GSH, reduced glutathione; TGPx, thioredoxin GPx-like peroxidase; GSSG, oxidized glutathione; BPTI, bovine pancreatic trypsin inhibitor; PDB, Protein Data Bank; BiFC, bimolecular fluorescence complementation; GST, glutathione *S*-transferase.

0022-2836/$ - see front matter © 2011 Elsevier Ltd. All rights reserved.

rather than for the formation of one disulfide bond plus harmful ROS. The question then arises: Has the system evolved to be inefficient or is the peroxide generated used productively?

Recently, we reported that hydrogen peroxide added to a folding protein or generated *in situ* could result in a relatively efficient oxidative refolding to the native state *in vitro*.[6] Hence, two disulfide bonds can be formed per molecule of molecular oxygen with no net production of harmful species. This process could occur either directly via the oxidation of a dithiol in the folding protein to a disulfide by peroxide or indirectly via protein disulfide isomerase (PDI) acting as an intermediary. Either way, as long as the peroxide was kept at submillimolar concentrations, refolding to the native state was efficient, with no observed oxidative side reactions.

Peroxide can be converted into disulfide bonds by other catalyzed mechanisms. Glutathione peroxidase (GPx) activity—the catalysis of the reaction of peroxide with reduced glutathione (GSH)—was first reported over 50 years ago.[7] The GPx family is found across archaea, prokaryotes, and eukaryotes, with eight human family members known.[8] The mechanisms of their action are complex.[9] However, it increasingly becomes clear that the family is a misnomer, as many family members are more efficient using other reductants than GSH, with thioredoxins probably representing the norm.[8,10]

Human GPx7 and GPx8 are currently annotated as secreted GPxs. Here, we show that both are actually located in the ER and associate with the peroxide-producing Ero1α. Furthermore, neither has significant GPx activity; instead, they have a preference for receiving electrons from PDI, another key player in the formation of native disulfide bonds[11] (i.e., they have PDI peroxidase activity). Hence, *in vitro*, the addition of PDI with GPx7 or GPx8 and peroxide to a reduced unfolded protein results in the very rapid attainment of the folded disulfide-bonded state. Furthermore, the addition of GPx7 to a mixture of purified Ero1α, PDI, and GSH resulted in a significant increase in oxygen consumption. Hence, the ER-resident PDI peroxidases GPx7 and GPx8 may represent a novel route for the productive use of peroxide produced by Ero1α during disulfide bond formation.

Results

Human GPx7 and GPx8 are ER-resident proteins

As part of a screen to find novel KDEL-like ER retrieval motifs,[12] we identified two human GPx family members (*GPX7* and *GPX8* gene products) as being potentially ER resident due to C-terminal –REDL and –KEDL motifs, respectively. The only report on the characterization of these proteins that we are aware of suggests that GPx7 has little detectable GPx activity *in vitro* and that it may play a role in alleviating oxidative stress from polyunsaturated fatty acids in breast cancer cells.[13] However, if GPx7 and GPx8 are located in the ER and possess GPx activity *in vivo*, then they could potentially provide a novel route by which peroxide generated by Ero1 during disulfide bond formation could be used productively.

GPx7 is 187 amino acids in length, with a predicted 19-amino-acid N-terminal cleavable signal sequence. In contrast, GPx8, which is 209 amino acids in length, is predicted to be a type I transmembrane protein, with a short N-terminal cytoplasmic region and with the putative catalytic domain located in the ER. Database analysis suggests that both proteins are widely expressed but at low transcriptional levels, similar to the profile observed for Ero1α. An alignment of GPx7 and GPx8 with other human GPxs (Fig. 1) reveals conservation of the catalytic residue (cysteine or selenocysteine) required for GPx activity (Cys57 and Cys79, respectively, for GPx7 and GPx8), but also that the loop required for tetramerization and the residues required to define glutathione specificity[8,10] are missing. This implies that both are probably members of the thioredoxin GPx-like peroxidase (TGPx)[8] family.

To examine the cellular localization of GPx7 and GPx8, we cloned the full-length gene products into the eukaryotic expression vector pRK7 with an HA-tag. Since these proteins include an N-terminal signal sequence or a transmembrane region, along with a C-terminal putative ER retrieval motif, the HA-tag had to be placed internally within the protein. We chose to place the tag 5 amino acids from the C-terminus (i.e., prior to the KDEL-like putative ER retrieval motif). Hence, the constructs made were M1-L182-HA-tag-K183-L187 for GPx7 and M1-K204-HA-tag-K205-L209 for GPx8. Immunofluorescence in transfected HeLa cells revealed a fine reticular network suggesting ER localization of the constructs. This localization was confirmed by co-staining the cells with antibodies against the ER marker PDI (Fig. 2a) and the Golgi marker GM130. Subsequently, polyclonal rabbit anti-protein antibodies were raised against both purified proteins (see the text below). Immunofluorescence using these antibodies showed that endogenous GPx8 in HeLa cells also shows ER localization (Fig. 2b). Unfortunately, immunofluorescence of endogenous GPx7 gave a very weak staining; hence, we were unable to determine if the endogenous protein is also ER located. To confirm that the putative N-terminal transmembrane region of GPx8 is not a cleavable signal sequence, we performed Western blot analysis after subcellular fractionation. The results (Fig. 2c) confirm that GPx8 is a transmembrane

```
GPx1 SVYAFSARPLAGGEPVSLGSLRGKVLLIENVASLUGTTVRDYTQMNELQRRLGPRGLVVLGFPCNQFGHQENAKNEEILNSLKYVRPGGGFEPNFM
GPx2 SFYDLSAISLDG EKVDFNTFRGRAVLIENVASLUGTTTRDFTQLNELQCRF PRRLVVLGFPCNQFGHQENCQNEEILNSLKYVRPGGGYQPTFT
GPx3 TIYEYGALTIDGEEYIPFKQYAGKYVLFVNVASYUGLTG QYIELNALQEELAPFGLVILGFPCNQFGKQEPGENSEILPTLKYVRPGGGFVPNFQ
GPx4 SMHEFSAKDIDG HMVNLDKYRGFVCIVTNVASQUGKTEVNYTQLVDLHARYAECGLRILAFPCNQFGKQEPGSNEEIKEFAA      GYNVKFD
GPx5 TIYDYEAIALNKNEYVSFKQYVGKHILFVNVATYCGLTA QYPELNALQEELKPYGLVVLGFPCNQFGKQEPGDNKEILPGLKYVRPGGGFVPSFQ
GPx6 TIYEYGALTLNGEEYIQFKQFAGKHVLFVNVAAYUGLAA QYPELNALQEELKNFGVIVLAFPCNQFGKQEPGTNSEILLGLKYVCPGSGFVPSFQ
GPx7 DFYDFKAVNIRG KLVSLEKYRGSVSLVVNVASECGFTDQHYRALQQLQRDLGPHHFNVLAFPCNQFGQQEPDSNKEIESFARRT     YSVSFP
GPx8 SFYAFEVKDAKG RTVSLEKYKGKVSLVVNVASDCQLTDRNYLGLKELHKEFGPSHFSVLAFPCNQFGESEPRPSKEVESFARKN     YGVTFP
                          *      ***  ▲          *  *           * *******  *                    *

GPx1 LFEKCEVNGAGAHPLFAFLREALPAPSDDATALMTDPKLITWSPVCRNDVAWNFEKFLVGPDGVPLRRYSRRFQTIDIEPDIEALLSQGPSCA
GPx2 LVQKCEVNGQNEHPVFAYLKDKLPYPYDDPFSLMTDPKLIIWSPVRRSDVAWNFEKFLIGPEGEPFRRYSRTFPTINIEPDIKRLLKVAI
GPx3 LFEKGDVNGEKEQKFYTFLKNSCPPTSE    LLGTSDRLFWEPMKVHDIRWNFEKFLVGPDGIPIMRWHHRTTVSNVKMDILSYMRRQAALGVKRK
GPx4 MFSKICVNGDDAHPLWKWMKIQPKGKGI                LGNAIKWNFTKFLIDKNGCVVKRYGPMEEPLVIEKDLPHYF
GPx5 LFEKGDVNGEKEQKVFSFLKHSCPHPSE    ILGTFKSISWDPVKVHDIRWNFEKFLVGPDGIPVMRWSHRATVSSVKTDILAYLKQFKTK
GPx6 LFEKGDVNGEKEQKVFTFLKNSCPPTSD    LLGSSSQLFWEPMKVHDIRWNFEKFLVGPDGVPVMHWFHQAPVSTVKSDILEYLKQFNTH
GPx7 MFSKIAVTGTGAHPAFKYLAQTS                        GKEPTWNFWKYLVAPDGKVVGAWDPTVSVEEVRPQITALVRKLILLKREDL
GPx8 IFHKIKILGSEGEPAFRFLVDSS                        KKEPRWNFWKYLVNPEGQVVKFWKPEEPIEVIRPDIAALVRQVIIKKKEDL
       *                    ──────────────────────      *** * *    *
```

Fig. 1. Alignment of human GPxs. The active-site cysteine/selenocysteine residues are indicated with an arrow, while the region involved in tetramerization and thought to give glutathione specificity to glutathione peroxides[8,10] is underlined. The nonhomologous N-terminal regions, which include the signal sequence of GPx7 and the transmembrane region of GPx8, are not shown.

protein, with bioinformatic analysis implying that the N-terminus of the protein is in the cytoplasm and, hence, the catalytic site is in the ER lumen.

GPx7 and GPx8 are not GPxs

In order to examine the *in vitro* enzymatic activities of GPx7 and GPx8, we cloned the mature form of GPx7 (Q20-L187) and the luminal domain of GPx8 (K38-L209) into a bacterial expression vector with an N-terminal hexa-histidine tag. The proteins were expressed in the cytoplasm of *Escherichia coli* and purified by immobilized metal affinity and ion-exchange chromatography to single species, as determined by Coomassie-stained SDS-PAGE gels. Purified GPx8 was well behaved in a wide range of buffers, while GPx7 had a tendency to form microaggregates under a variety of conditions, making it less amenable for detailed biophysical studies.

The classic assay for GPx activity determination is coupling the production of oxidized glutathione (GSSG) to a more significant absorbance change using glutathione reductase.[14] This reduces GSSG to GSH using NADPH as the electron donor, with a concomitant reduction in absorbance at 340 nm. With this assay, GPx7 and GPx8 were shown to have a very low GPx activity (<0.01% of the relative activity of bovine GPx1; Fig. 3a). Indeed, human PDI has a higher GPx activity than either GPx7 or GPx8 (Fig. 3b). However, GPx7 and GPx8 lack the loop in GPxs that determines glutathione specificity (Fig. 1), suggesting that both may be members of the TGPx family.[8] The only known thioredoxin superfamily members present in the ER are the PDI family members. Hence, GPx7 and GPx8 are possible PDI peroxidases that catalyze the reaction:

$$PDI_{reduced} + H_2O_2 \rightarrow PDI_{oxidized} + H_2O$$

To examine this possibility, we repeated the assay for GPx7 and GPx8 in the presence of PDI. As noted above, PDI by itself has GPx activity (Fig. 3b), as the active sites in the two catalytic domains can be oxidized to the disulfide state by peroxide ($k = 9.2\ M^{-1}\ s^{-1}$)[6] and can be reduced to the dithiol state by GSH (k on the order of $200\ M^{-1}\ s^{-1}$).[15] Given the relative rates of these two reactions, the oxidation of PDI by peroxide is rate limiting in this assay. When GPx7 or GPx8 and PDI were combined, the rate of formation of GSSG was faster than the

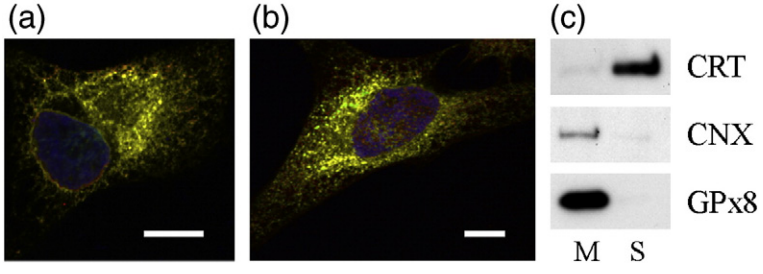

Fig. 2. Subcellular localization of human GPx7 and GPx8. (a) Immunofluorescence localization of HA-tagged GPx7. Merged image of PDI staining (green) and GPx7 staining (red). HA-tagged GPx8 showed a similar ER localization. (b) Immunofluorescence localization of endogenous GPx8. Merged image of PDI staining (green) and GPx8 staining (red). The scale bars in (a) and (b) represent 10 μm. (c) A Western blot analysis after subcellular fractionation was performed to confirm that GPx8 is a transmembrane protein. Calreticulin (CRT) is the control for soluble ER protein, and calnexin (CNX) is the control for transmembrane ER protein. M, endomembrane fraction; S , soluble ER fraction.

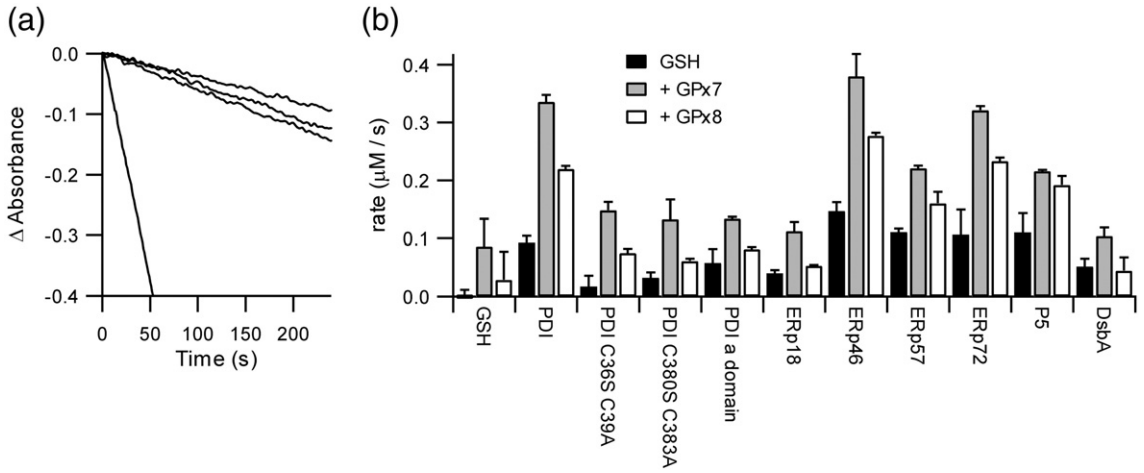

Fig. 3. Human GPx7 and GPx8 are not GPxs. (a) Change in absorbance at 340 nm as a function of time in the coupled GPx assay. Mature GPx7 or the luminal domain of GPx8 gives traces only slightly faster than the noncatalyzed reaction. Top to bottom: The traces are noncatalyzed, and GPx8 (20 μM), GPx7 (20 μM), and bovine GPx1 (20 nM) catalyzed. (b) Rates of NADPH consumption per second in the coupled GPx activity assay. The data are expressed as average ± SD ($n = 2–5$), with the noncatalyzed rate subtracted. When present, [GPx7 or GPx8] = 20 μM, [PDI, mutants, **a** domain, ERp72, ERp18, ERp46, ERp57, P5, or DsbA] = 10 μM. For both panels, [GSH] = 0.5 mM and [peroxide] = 0.3 mM.

sum of the two individual processes (Fig. 3b). This implies that the combined rate of oxidation of GPx7/GPx8 by peroxide and the subsequent oxidation of PDI by the oxidized state of GPx7/GPx8 are faster than the single step of the oxidation of PDI by peroxide. Given the relative concentrations of GSH (0.5 mM) and PDI (10 μM) in this assay, this result also implies that the second-order rate constant for the reaction of GPx7 and GPx8 with PDI is at least 50-fold higher than their rate of reaction with GSH. Hence, while both GPx7 and GPx8 are not efficient GPxs, they are both PDI peroxidases. This was confirmed by concentration dependence studies (see Supplementary Results), which implied that GPx7 is at least 95-fold more efficient with PDI than with GSH and that GPx8 is at least 250-fold more efficient with PDI than with GSH.

PDI has two catalytic domains: **a** and **a′**.[11] Mutating the active-site residues in each active site in mature human PDI showed that both contribute to the GPx activity of PDI and to activity in the GPx7 or GPx8 coupled assay (Fig. 3b). This suggests that GPx7 and GPx8 may interact with either catalytic domain of PDI; however, it should be noted that this assay is an indirect measure, since it is coupled to the GSH reduction of the oxidized active site of PDI and hence to the reduction of the GSSG produced by glutathione reductase. The isolated **a′** domain of human PDI is unstable and, hence, unsuitable for testing in this assay, but the isolated **a** domain is stable and shows no synergy of action with GPx7 or GPx8 compared with the sum of the independent rates (Fig. 3b), implying that other domains are required for the interaction with GPx7/GPx8.

PDI is the archetypal member of the ER-resident PDI family. It is possible that other catalytically active members of the family may be the natural partners of GPx7 and GPx8 *in vivo*. To test for this possibility, we examined the activity of GPx7 and GPx8 in the coupled assay with the human PDI family members ERp18, ERp46, ERp57, ERp72, and P5 and with the prokaryotic thiol disulfide oxidoreductase DsbA (Fig. 3b). While the single-domain enzyme ERp18[11] showed no synergy of action with GPx7 or GPx8, the other human PDI family members showed activity with both GPx7 and GPx8, although there were very clear differences in activity, with PDI, ERp72, and ERp46 having higher activity than ERp57 and P5. While the functional characterization of these human PDI family members is far from complete, one notable difference between the family members is that ERp57, which shares the same domain architecture as PDI, is significantly less effective with GPx7 or GPx8. ERp57 and PDI differ in substrate specificity due mainly to differences in their substrate binding **b′** domains.[11] It is therefore possible that this is also reflected in their ability to interact with GPx7 and GPx8.

Stopped-flow kinetics for the peroxide oxidation of GPx8

Previously, we have determined the rate of reaction of peroxide with the catalytic site in the **a** domain of PDI using a change in the intrinsic fluorescence of the protein.[6] Examination of the sequence of GPx7 and GPx8 reveals that both contain three tryptophan residues, with one W142

(GPx7) or W164 (GPx8) conserved in the GPx family (Fig. 1) and located close to the active site (see the text below for structure determination). Since GPx8 is more amenable to biophysical characterization, we chose to study whether redox state-dependent changes in fluorescence could be observed in it. When peroxide was added to reduced GPx8, a time-dependent decrease in fluorescence was observed, consistent with W164 acting as a spectroscopic marker for the redox state of the active site. The changes in fluorescence were complex, especially at peroxide concentrations greater than 20 mM (Fig. 4a); however, at peroxide concentrations up to 100 mM, a rapid initial decrease in fluorescence could be fitted to a single exponential function (Fig. 4b) with random residuals. The rate constant for this reaction was linearly dependent on the concentration of peroxide (Fig. 4c), consistent with a pseudo-first-order reaction. This suggests that the reaction being observed is the formation of the active-site cysteine sulfenic acid. From the linear dependence of the rate constant on peroxide concentration over the range 0–100 mM, a second-order rate constant of $95 \pm 1\ M^{-1}\ s^{-1}$ was obtained, which was 10-fold greater than that for the reaction of PDI with peroxide ($9.2\ M^{-1}\ s^{-1}$).[6]

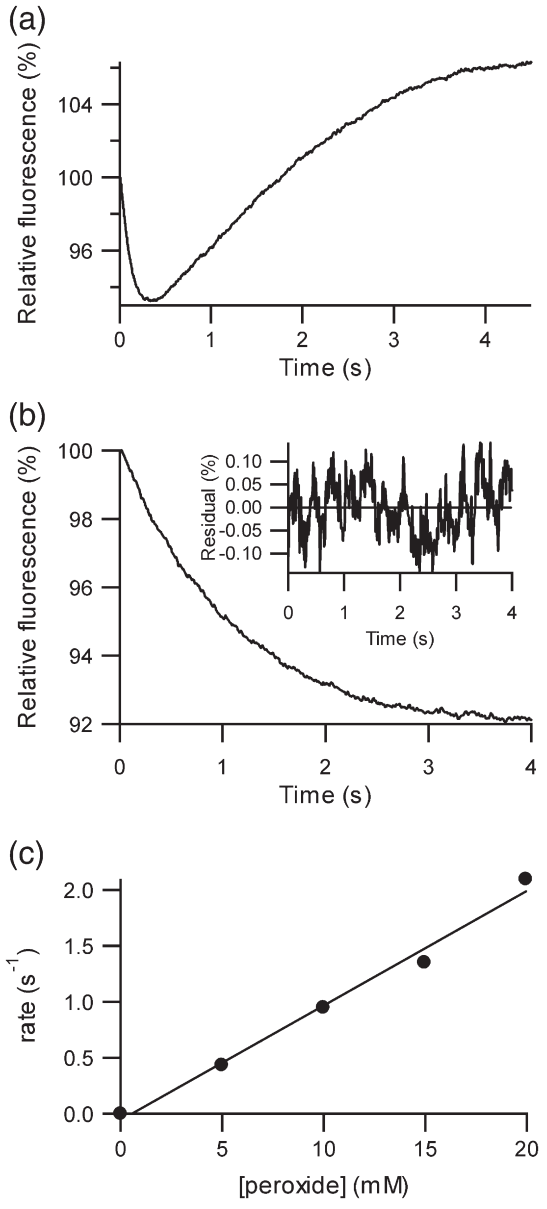

Fig. 4. Kinetics of changes in the fluorescence of the luminal domain of GPx8 upon oxidation. (a) Representative trace of time-dependent changes in the fluorescence of GPx8 upon addition of 100 mM H_2O_2. The initial reaction up to 0.25 s fits well to a pseudo-first-order reaction (see the text below). The subsequent kinetics are more complex. However, they are consistent with a slower intermolecular event such as the formation of an active-site cysteine sulfinic acid or the formation of a Cys108 sulfinic acid or a methionine sulfoxide. This is consistent with preliminary data indicating that both GPx7 and GPx8 are irreversibly inactivated by prolonged incubation in peroxide. (b) Representative trace of the kinetics of oxidation in the presence of 10 mM hydrogen peroxide. Inset: The residuals from fitting to a single exponential function. (c) Linear dependence of the pseudo-first-order rate constant of oxidation of GPx8 on the concentration of peroxide ($n = 3$–4). At all concentrations of peroxide examined, the kinetics showed random residuals to a single exponential function when an appropriate time frame was used.

GPx7 and GPx8 combined with PDI are efficient for peroxide-mediated oxidative protein folding

We have recently shown that the widely studied model for oxidative protein folding, protein bovine pancreatic trypsin inhibitor (BPTI), is able to fold to the native three-disulfide-bonded state using hydrogen peroxide as the electron acceptor in disulfide bond formation.[6] Consistent with this, a mass spectrometry-based analysis of the refolding of BPTI using *in situ* generated peroxide showed the initial disappearance of the reduced species; the appearance and subsequent disappearance of the one-disulfide-containing and subsequently of the two-disulfide-containing folding intermediates; and finally, the appearance of the native three-disulfide-containing species (Fig. 5). For the uncatalyzed reaction, the pseudo-first-order rate constant for the disappearance of reduced species was $0.15 \pm 0.01\ min^{-1}$, with 50% appearance of the three-disulfide species after approximately 30 min (Fig. 5a). The addition of catalytic amounts of PDI results in a slight increase in the initial rate disulfide bond formation in BPTI to $0.34 \pm 0.05\ min^{-1}$, consistent with the relative rates of peroxide oxidation of PDI ($9.2\ M^{-1}\ s^{-1}$)[6] and BPTI ($5\ M^{-1}\ s^{-1}$).[6] However, PDI is able to efficiently catalyze intramolecular disulfide bond rearrangement in BPTI,[11]

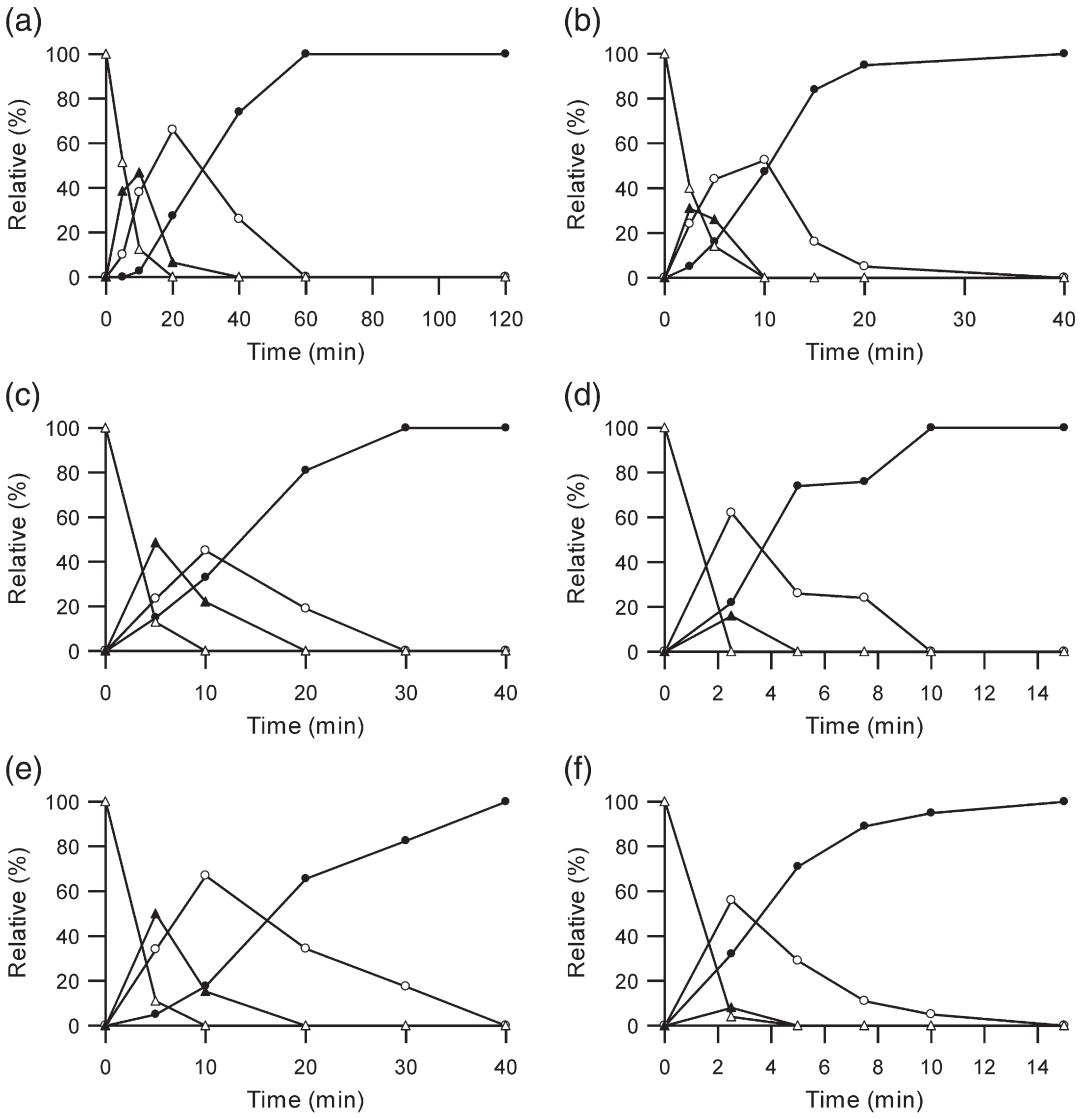

Fig. 5. BPTI refolding. Representative traces for variations in the rate of disulphide bond formation in 50 μM BPTI using 50 nM glucose oxidase and 10 mM glucose to generate peroxide as an oxidant, as analyzed by electrospray ionization mass spectrometry. (a) Noncatalyzed refolding; (b) with 7 μM PDI; (c) with 7 μM GPx7; (d) with 7 μM GPx7 and PDI; (e) with 7 μM GPx8; (f) with 7 μM GPx8 and PDI. Filled circles , three disulfides; open circles , two disulfides; filled triangles , one disulfide; open triangles , fully reduced. Note the different timescales on the *x*-axis in (a)–(f).

and this aids the formation of the native three-disulfide state, resulting in an average half time for the appearance of this state of 9 min (Fig. 5b).

When catalytic amounts of GPx7 or GPx8 were added to refolding BPTI, again the initial rate of oxidation was slightly faster than the uncatalyzed reaction (Fig. 5c and e), with a pseudo-first-order rate constant for the disappearance of reduced species of 0.38 ± 0.06 min^{-1} and 0.40 ± 0.06 min^{-1}, respectively, and with 50% appearance of the three-disulfide species after 15–17 min. However, the overall effects were not dramatic. Given the relative rates of oxidation of GPx8 (95 M^{-1} s^{-1}) and BPTI (5 M^{-1} s^{-1})[6] with peroxide, this approximately 2-fold increase in the rate of disappearance of reduced BPTI implies that the oxidation of BPTI by GPx8 is probably rate limiting in this reaction. Hence, GPx7 and GPx8 are able to directly oxidize folding proteins, but not efficiently, consistent with their being TGPx family members.

In contrast to the addition of single components, when both PDI and GPx7 or GPx8 were present in the refolding assay, an additive effect was seen (Fig. 5d and f) with an increase in the initial rate of disulfide bond formation in BPTI, such that little or no fully reduced species was present at the first time

point (i.e., rates too fast to measure accurately in this assay format) and a time taken for 50% of the BPTI to reach the native state of approximately 4 min. These results are consistent with GPx7 and GPx8 being efficient PDI peroxidases.

Crystal structure of human GPx8

The structures of proteins greatly aid in their functional characterization; hence, we aimed to determine the high-resolution structures of GPx7 and GPx8. During our initial screening, crystals of mature human GPx7 were obtained, but they diffracted poorly, and optimization was curtailed by the deposition of the crystal structure of the protein to 2.0 Å by the Structural Genomics Consortium [Protein Data Bank (PDB) file 2P31]. In contrast to our trials with GPx7, diffracting crystals of the luminal domain of human GPx8 (K38-L209) were rapidly obtained, and the crystal structure was refined to 1.8-Å resolution. A summary of crystallographic parameters and refinement statistics is given in Table 1. There are three monomers per asymmetric unit (Fig. 6a). The N-terminal His-tag (MHHHHHHM), the first N-terminal residue of the mature protein (K38) of chains A–C, and the three C-terminal residues (D207–L209) of chain C were not seen in the electron density map.

The protein structure exhibits the typical extended thioredoxin fold (βββαβαβαββα) exhibited by GPx family members.[8] It consists of four α-helices located at the protein surface, two β-strands located at the protein surface, and a central five-stranded mixed β-sheet. The active-site cysteine of GPx8 is located at the beginning of α1. Like human GPx4 and GPx7, GPx8 lacks a 24-residue surface-exposed loop (Fig. 6b) located between α3 and β6, which is present in other human GPx isoforms (GPx1, GPx2, GPx3, and GPx5), involved in tetramerization, and thought to be involved in glutathione specificity (see the text above). After our acquisition of the structure of mature human GPx8, the crystal structure of a slightly shorter construct of human GPx8 (I44-L209) was determined by the Structural Genomics Consortium to 2.0-Å resolution (PDB file 3CYN). No significant differences were found between this lower-resolution structure and our structure.

Table 1. Crystallographic statistics of the structure of the nonlabeled mature human GPx8 grown at pH 6.0, as processed by XDS

Data collection statistics	
Space group	$C1_21$
Unit cell parameters: *a*, *b*, *c* (Å)	90.43, 122.30, 70.18
Temperature (K)	100
Wavelength (Å)	0.89997
Resolution (Å)	66–1.8
R_{merge} (%)	7.1 (26.4)
Completeness (%)	99.3 (99.5)
$I/\sigma I$	16.0 (5.7)
Unique reflections	61,998 (9242)
Redundancy	5.0 (5.1)
Mosaicity (°)	0.28
B-factor from Wilson plot (Å^2)	20.7
Refinement statistics	
Resolution (Å)	20–1.8
Total no. of reflections	58,897
R-factor (%)	20.8
R_{free} (%)	24.9
Protein atoms (A, B, C, D)	4246
Water atoms	534
SO_4^{2-} atoms	5
Geometry statistics	
RMSD of bond distance (Å)	0.0133
RMSD of bond angle (°)	1.37
RMSD *B*	
Main-chain bonded atoms (Å^2)	0.81
Side-chain bonded atoms (Å^2)	2.24
Main-chain angle (Å^2)	1.42
Side-chain angle (Å^2)	3.63
Average *B*	
Main-chain atoms (Å^2)	13.2
Side-chain atoms (Å^2)	15.7
Water molecules (Å^2)	28.2
Sulfate atoms (Å^2)	45
Ramachandran plot	
Most favored region (%)	99.2
Additionally allowed regions (%)	0.8
Disallowed regions (%)	0

The values in parentheses are for the highest-resolution shell.

GPx7 and GPx8 interact with Ero1α *in vivo* and modulate Ero1α activity *in vitro*

While several processes generate hydrogen peroxide in the ER lumen (e.g., the final step of ascorbate biosynthesis),[16] the route thought to be the most potentially harmful to the organism is the production of peroxide by Ero1 family members during the catalyzed formation of disulfide bond. Hence, it would make sense for human GPx7 and/or GPx8 to be physically associated with Ero1α and/or Ero1β to immediately utilize the peroxide made rather than let it diffuse away. To test this hypothesis, we undertook a range of coimmunoprecipitation experiments using a variety of cell lines. However, neither endogenous proteins nor tagged heterologously expressed proteins were observed to coimmunoprecipitate. Since there are numerous possible reasons for false-negative results, we focused on potential interactions detected by bimolecular fluorescence complementation (BiFC), a technique developed to look at transient interactions, as BiFC can be used to both quantify the interaction and identify the cellular localization of the interaction.

Mature human GPx7, Ero1α, and Ero1β, along with the luminal domain of human GPx8, were cloned into previously generated BiFC vectors.[17] These vectors result in the proteins being tagged with either the N-terminal Y1 fragment or the C-

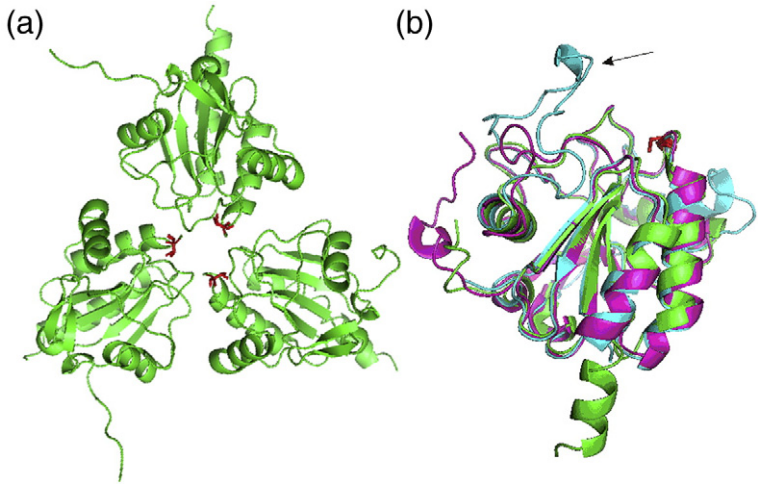

Fig. 6. Crystallographic analysis of GPx8. (a) Crystal structure of human mature GPx8 at 1.8 Å showing the three molecules in a symmetric unit. The active-site cysteine is shown in red. (b) Superimposed structure of human mature GPx8 (green), GPx4 (pink), and GPx1 (cyan). The active-site cysteines are shown in red. Note the large loop (marked with arrow) present in GPx1, but not in GPx4 or GPx8.

terminal Y2 fragment of yellow fluorescent protein and targeted to the ER using the calreticulin signal sequence. Both GPx7 and GPx8 gave BiFC fluorescence signals with Ero1α that were significantly above the Y1 + Y2 negative control, as seen by flow cytometric analysis (Fig. 7a). As a further control, combinations of 31 ER-resident proteins implicated in protein folding were tested in duplicate by BiFC for interaction *in vivo*, with a parallel Western blot analysis to confirm the expression levels of the Y1 and Y2 fusion proteins. Of the 257 combinations tested, 29 (11%) gave positive results at least three times higher than the Y1 + Y2 negative control (data not shown). Of the 8 combinations tested for GPx7 and of the 8 combinations tested for GPx8, only Ero1α gave positive BiFC results. Of the 31 combinations tested for Ero1α, 9 gave positive results, including GPx7, GPx8, and 5 PDI family members. Of the 31 combinations tested for the PDI family member P5 and of the 8 combinations tested for PDIp, only Ero1α gave positive results. The results from this large screen suggest a specific interaction of GPx7/GPx8 with Ero1α. Visualization of the BiFC signals from Ero1α and GPx7 or GPx8 showed the appearance of a fine reticular network suggesting interaction in the ER, and this was confirmed by co-staining with a calreticulin antibody (Fig. 7b). Similar trials using Ero1β did not give BiFC signals, but a parallel Western blot analysis showed negligible expression levels of the Y1 or Y2-Ero1β fusion proteins.

While BiFC suggested that there is a physical association between Ero1α and both GPx7 and GPx8 *in vivo*, we wanted to see if there was a functional interaction. Since any peroxide produced by Ero1α can be utilized directly to oxidize dithiols to disulfides in folding proteins or can be mediated by PDI, the PDI peroxidases should be viewed as facilitators, making this process more efficient but not essential. Hence, we thought that the *in vivo*

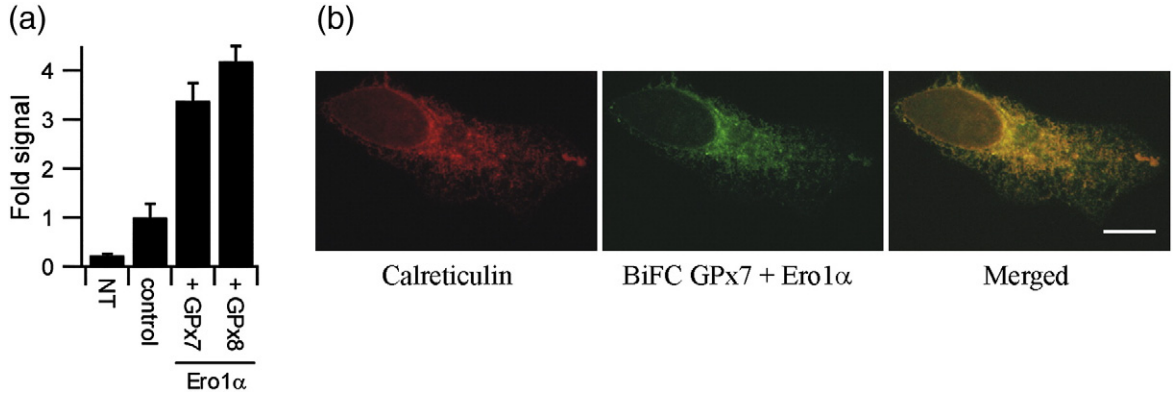

Fig. 7. GPx7 and GPx8 interact with Ero1α *in vivo*. (a) Quantification of the fluorescence signal from BiFC relative to the Y1 + Y2 control. Data are expressed as mean ± SD ($n = 4$; each sample counts 3000 cells). NT , nontransfected cells. (b) BiFC localization of the interaction of GPx7 and Ero1α by fluorescence microscopy. Calreticulin is used as an ER marker. The scale bar represents 10 μm. A similar localization was observed for GPx8–Ero1α interactions.

confirmation of a role would be problematic. However, it would also make sense if the interaction of GPx7 and/or GPx8 directly modulated the oxidase activity of Ero1α such that the rate of peroxide generation increased when these peroxide-utilizing facilitators were present. To test this hypothesis, we examined the rate of oxygen consumption of Ero1α *in vitro*. When PDI and GSH are present, Ero1α uses molecular oxygen to oxidize the active sites of PDI, which are then reduced by GSH. Ero1α turnover can be directly monitored by a decrease in oxygen concentration in the solution using an oxygen electrode. After an initial short lag period, the rate of oxygen consumption by Ero1α is linear and dependent on the presence of PDI (Fig. 8a). When GPx7 or GPx8 is added to the reaction, the rate of oxygen consumption is increased (Fig. 8a). While the increase for GPx8 is small, oxygen consumption by Ero1α when GPx7 and PDI are present is 31% greater than in the absence of GPx7 and is significantly different ($p<0.05$). This effect is dependent on the presence of PDI in the reaction (Fig. 8b). Hence, Ero1α only oxidizes PDI and not GPx7 or GPx8, but the rate of this oxidation of PDI by Ero1α is increased in the presence of PDI peroxidases, especially GPx7. This implies that there is a functional interaction between these proteins.

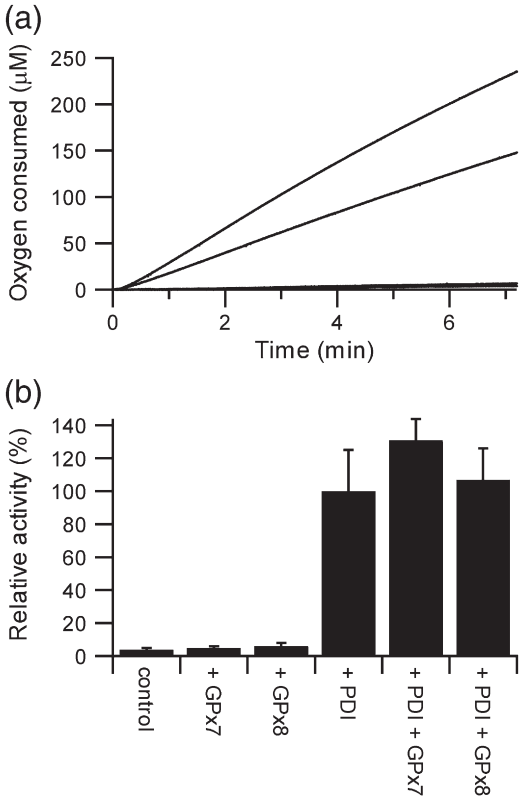

Fig. 8. *In vitro* Ero1α activity is influenced by the presence of GPx7 and GPx8. Oxygen consumption was monitored with an oxygen electrode immediately after the injection of Ero1α into PDI, with GSH as reducing equivalent. (a) The rate of oxygen consumption by Ero1α depends on the presence of PDI and is increased by the concomitant presence of GPx7. Top to bottom: The four traces are Ero1α+GPx7+PDI, Ero1α+PDI, Ero1α alone, and PDI alone. Note that the bottom two traces are nearly superimposed and have very low rates of oxygen consumption. (b) The increase in oxygen consumption by Ero1α in the presence of GPx7 or GPx8 depends on the presence of PDI in the reaction.

Discussion

The major route for disulfide bond formation in the ER is thought to be via the action of Ero1 family members. These enzymes generate hydrogen peroxide as a by-product of disulfide bond formation *in vitro* and *in vivo*.[1–3] This production of peroxide is not only potentially harmful to the cell, but it is also a nonefficient use of resources if peroxide is not utilized, since there is the potential to generate two disulfides per molecule of molecular oxygen. Recently, it has been elegantly demonstrated that disulfide bond formation *per se* does not generate oxidative stress, while induction of the unfolded protein response does.[18] This implies that cells either have extremely efficient mechanisms in the ER to remove the peroxide produced by Ero1 or utilize peroxide in some way. We have demonstrated *in vitro* that peroxide can be efficiently utilized to make native disulfide bonds in a folding protein with no significant oxidative side reactions so long as the peroxide concentration is kept at submillimolar concentrations.[6] This productive folding can occur either via the direct reaction of peroxide with a free thiol group on the folding protein to form a cysteine sulfenic acid with subsequent formation of disulfide bonds or via the action of a protein folding catalyst such as PDI.

Here, we demonstrate *in vitro* a novel pathway for utilizing the peroxide generated by Ero1 for native disulfide bond formation. We show that two human GPx family members previously annotated as being potentially secreted are in fact ER resident and have minimal GPx activity. Instead, both are members of the TGPx family and, hence, have PDI peroxidase activity *in vitro* and presumably *in vivo*. The addition of either GPx7 or GPx8 to a mixture of reduced denatured protein, PDI, and peroxide resulted in rapid oxidative folding. Furthermore, the addition of human GPx7 significantly increases the rate of oxygen consumption by human Ero1α, suggesting a functional and/or physical interaction and that these PDI peroxidases could directly utilize Ero1-produced peroxide.

There are other potential pathways for the productive utilization of peroxide in the ER of human cells. For example, the human two-cysteine

peroxiredoxin family member Prx IV has been shown to be an ER-resident protein[19] and has been recently reported to protect cells by removing peroxide produced during disulphide bond formation.[20] During the preparation of this article, it was reported that Prx IV feeds into productive disulfide bond formation *in vitro* and *in vivo*,[21] since it must be reduced to complete the catalytic cycle; in the ER, this is performed by PDI family members.[22] The peroxidase activity of Prx IV could be a system parallel to the PDI peroxidases, or as originally suggested by Tavender *et al.*, it could function as a redox-dependent molecular chaperone.[19] It is noteworthy that *in vitro* data[21] show that the oxidation of a substrate protein to the native state by Prx IV + PDI + peroxide is significantly slower than that reported here for GPx7 or GPx8 + PDI (Fig. 5d and f), at least in part due to the slower rates of oxidation of PDI by peroxide-oxidized Prx IV (compared with GPx7 or GPx8). While the assay systems were not identical, this suggests that the PDI peroxidases are at least as efficient as Prx IV at feeding peroxide into productive disulfide bond formation.

Any pathway to remove or utilize peroxide must be efficient, and such efficiency is perhaps best achieved by juxtaposing the utilizing enzyme with the source (i.e., Ero1). This may already happen in the simplest version of the system. Ero1 only makes peroxide when it oxidizes the active site of PDI. However, PDI has two active sites, and if both are reduced, then the mixed disulfide complex Ero1–PDI formed during the catalytic cycle may juxtapose the second active site of PDI with the site of peroxide production. The high local concentration would then increase the probability of oxidation of the second active site by the peroxide. It is tempting to speculate that this may be the major route in *Saccharomyces cerevisiae*, which lacks ER-resident peroxiredoxins and GPx or TGPx family members and which has a much smaller number of PDI family members. Humans have around 20 PDI family members,[11] and several of these, including ERp18, have been reported to form mixed disulfides with Ero1α.[23] Oxidation of single active-site species such as ERp18 would require an alternative mechanism for peroxide utilization. Furthermore, given the much greater generation time for humans compared with yeast, the requirement for the efficiency of peroxide removal or utilization may be greater. If endogenous GPx7 and GPx8 physically and functionally interact with Ero1α (as suggested by our *in vivo* BiFC results) and modulate its activity, as suggested by our *in vitro* results, then this, combined with the higher reactivity of these enzymes to peroxide compared with the active sites of PDI, would generate the required mechanisms. Either way, the catalytic activity of PDI, GPx7, GPx8, and Prv IV, combined with the absence of a catalase or a similar enzyme from the ER and with the lack of oxidative stress due to disulfide bond formation,[18] strongly suggests that the ER productively utilizes any peroxide produced during disulfide bond formation for disulfide bond formation.

Materials and Methods

Vector construction

Expression vectors for mature PDI, the **a** domain of PDI, mature ERp57, mature P5, mature ERp72, and mature BPTI were constructed previously.[24,25] The genes for human GPx7, GPx8, Ero1α, Ero1β, ERp29, ERp44, and TMX were cloned by PCR from IMAGE clones 3628580, 7472098, 3868538, 4829502, 8068999, 3934201, and 5740203, respectively.

BiFC vectors targeted to the ER were previously made[17] according to the design of Nyfeler *et al.*,[26] with the Q69M mutation introduced into the Y1 fragment to reduce the environmental sensitivity of fluorescence.[27] Constructs expressing mature Ero1α, Ero1β, GPx7, and the luminal domain of GPx8 were subcloned into these vectors.

Mutagenesis of plasmids was carried out using the QuikChange site-directed mutagenesis kit (Stratagene) according to the manufacturer's instructions.

Plasmid purification was performed using the QIAprep spin miniprep kit (Qiagen) and purification from agarose gels was performed using the gel extraction kit (Qiagen), both according to the manufacturer's instructions.

All plasmids generated were sequenced to ensure there were no errors in the cloned genes (see Table 2 for plasmid names and details).

Subcellular localization

The method of Raykhel *et al.* was used for the immunofluorescence localization of GPx7 and GPx8 in HeLa cells.[12] To determine whether GPx8 is a transmembrane protein, we used the protocol of Olivari *et al.*[28]

Protein purification

Human PDI, **a** domain, ERp72, ERp18, ERp57, P5, ERp46, and DsbA were purified by immobilized metal affinity chromatography and ion-exchange chromatography, as described previously for the **a** domain of PDI.[29] All of these proteins have an additional MHHHHHHM N-terminal hexa-histidine tag. BPTI was purified as described previously.[30] Pure reduced BPTI was lyophilized and resuspended into 10 mM HCl (pH 2.0) to prevent oxidative refolding. The concentrations of proteins were calculated based on their calculated molar extinction coefficients at 280 nm. All purified proteins were analyzed for authenticity by matrix-assisted laser desorption/ionization-time of flight mass spectrometry, and all experimentally determined masses were the same as the expected mass (within the mass accuracy limit of the spectrometer). For oxygen consumption assays, recombinant mature full-length human Ero1α and PDI proteins were purified as described previously.[31] After the cleavage of the glutathione *S*-transferase (GST) tag, the

Table 2. Vectors reported in this study

Plasmid	Basis	Protein produced
pOLR130	pET23	MH_6M-mature human PDI (Asp18-Leu508) with silent mutations to remove internal XhoI sites and with SpeI site added to the multicloning site
pOLR146	pET23	MH_6M-mature human PDI (Asp18-Leu508) Cys36S, Cys39A
pOLR147	pET23	MH_6M-mature human PDI (Asp18-Leu508) Cys380S, Cys383A
pLWRP69	pET23	MH_6M-PDI **a** domain (Asp18-Ala136)
pHIA128	pET23	MH_6M-mature human ERp18 (Ser24-Leu172)
pHIA282	pET23	MH_6M-mature human Erp46 (Arg33-L432) with silent mutations to remove internal NdeI site; R354K natural variant
pKEHS69	pET23	MH_6M-mature human ERp57 (Ser25-Leu505) with SpeI site added to the multicloning site
pHIA64	pET23	MH_6M-mature human ERp72 (Val20-Leu645)
pHIA43	pET23	MH_6M-mature P5 (Leu20-Leu440); K214R natural variant
pAKL122	pET23	MH_6M-mature *E. coli* DsbA (Ala19-Lys207)
pARK32	pET23	MH_6M-mature BPTI (Arg36-Ala93)
pKEHS780	pET23	MH_6M-mature human GPx7 (Q20-L187)
pKEHS767	pRK7	GPx7 full length with HA-tag inserted five amino acids from the C-terminus
pVD140	pRK7	GPx7 M1-L182-HA-tag-K183-L187
pVD54	pET23	MH_6M-luminal domain of human GPx8 (K38-L209)
pKEHS768	pRK7	GPx8 full length with HA-tag inserted five amino acids from the C-terminus
pFH56	pcDNA3.1	CRTss + EYFP1
pFH57	pcDNA3.1	CRTss + EYFP2
pARK38	pcDNA3.1	CRTss + EYFP1 + mature GPx7
pARK39	pcDNA3.1	CRTss + EYFP2 + mature GPx7
pARK40	pcDNA3.1	CRTss + EYFP1 + luminal domain GPx8
pARK41	pcDNA3.1	CRTss + EYFP2 + luminal domain GPx8
pARK42	pcDNA3.1	CRTss + EYFP1 + mature Ero1α
pARK35	pcDNA3.1	CRTss + EYFP2 + mature Ero1α
pARK37	pcDNA3.1	CRTss + EYFP1 + mature Ero1β
pARK36	pcDNA3.1	CRTss + EYFP2 + mature Ero1β
His6 PDI	pQE30	MRGSH_6GS-mature human PDI (Asp18-Leu508)
GST Ero1α	pGEX-6P-1	GST-mature human Ero1α (Glu24-His468) cleavable fusion

Expression from pET23 plasmids is induced with IPTG. CRTss , signal sequence of calreticulin; EYFP1 , N-terminal fragment of enhanced yellow fluorescence protein (Met1–Gln158; Q69M) for BiFC measurements; EYFP2 , C-terminal fragment of enhanced yellow fluorescence protein (Lys159–Lys239) for BiFC measurements. Excluding BPTI and DsbA, all proteins are human in origin.

Ero1α protein has the additional sequence GPLGS at the N-terminus.

GPx activity measurements

GPx activity was measured at pH 7.3 using a coupled assay following the decrease in absorbance at 340 nm due to the consumption of NADPH by glutathione reductase, as described previously,[6] with the reaction being started by the addition of H_2O_2. A molar extinction coefficient of 6200 M^{-1} cm^{-1} for NADPH[32] was used in the calculations.

BPTI refolding

Reduced and denatured BPTI (50 μM) was refolded at pH 7 in 0.1 M Na-phosphate buffer containing 1 mM ethylenediaminetetraacetic acid (EDTA), 10 mM glucose, and 50 nM glucose oxidase. The concentration of PDI, GPx7, and GPx8 was 7 μM. The refolding aliquots were alkylated with 1.1 M iodoacetamide and immediately loaded into Ni-NTA spin columns (Qiagen) to separate BPTI from hexa-histidine-tagged GPx7 and GPx8. Ni-NTA spin columns were preequilibrated with buffer containing 50 mM NaH_2PO_4, 300 mM NaCl, and 10 mM imidazole at pH 8. After loading, the column was washed once with washing buffer [50 mM NaH_2PO_4, 300 mM NaCl, and 20 mM imidazole (pH 8)]. The flow-throughs from the loading and washing steps were combined and purified before electrospray ionization mass spectrometry with the PepClean C-18 Spin Columns (Pierce). It should be noted that different folding intermediates of a protein can potentially show bias in their detection by electrospray ionization mass spectrometry; therefore, the results should be treated as though they are only semiquantitative.

Kinetics of GPx8 oxidation followed by stopped-flow fluorescence

Purified GPx8 was reduced by reaction with a 5-fold molar excess of DTT for 30 min at room temperature. After reduction, the protein was buffer exchanged into the stopped-flow reaction buffer [0.2 M Na-phosphate, 0.2 M citrate, 0.2 M borate, and 1 mM EDTA (pH 7.0)] using Biomax ultrafree centrifugal filter concentrators (Millipore). The rate of oxidation of the active site of GPx8 was determined by the decrease in tryptophan fluorescence using a KinTek SF-2004 stopped-flow fluorometer with an excitation of 280 nm and a bandpass emission of >320 nm at 25 °C, 10 μM reduced GPx8 with 5–100 mM H_2O_2, and preequilibration at 25 °C for 3 min.

Crystallization, structure determination, and refinement

Crystals of mature human GPx8 were obtained after 1 week via the sitting-drop vapor diffusion equilibration method using 2 μl of protein solution (10 mg/ml) and 2 μl

of well solution [2.5 M ammonium sulphate and 0.1 M 2-(*N*-morpholino)ethanesulfonic acid buffer (pH 6)] at 22 °C. Crystals were harvested, placed on paraffin oil for a few seconds, and then frozen in liquid nitrogen. The X-ray data of a single crystal were collected with a CCD detector at beamline X12 (DESY, Hamburg, Germany) in a nitrogen stream at 100 K at a wavelength of 0.89997 Å. Images were processed using the XDS program package.[33] The initial phase was determined from the molecular replacement solution obtained with PHASER (Phaser_MR) using the crystal structure of selenocysteine in the glycine mutant of human GPx 4 (PDB file 2gs3), which was treated with the CHAINSAW[34] program of the CCP4 program suite. The model was manually built in Coot.[35] The resulting model was refined using REFMAC5.[36] The data collection statistics and refinement statistics of the structure are given in Table 1.

Bimolecular fluorescence complementation

The method of Raykhel *et al.* was used for BiFC, with the yellow fluorescence of 3000 cells analyzed with a CyFlow flow cytometer (Partec) for each sample.[12] Transformation with the single plasmid controls resulted in transfected cells whose fluorescence intensity could not be distinguished from that of the nontransfected cell population.

Oxygen consumption assay

Oxygen consumption was measured using an Oxygraph-Clark-type oxygen electrode (Hansatech Instruments), as described previously.[31] All experiments were performed at 25 °C in 100 mM Tris–HAc, 50 mM NaCl, 1 mM EDTA, and 10 mM GSH (pH 7.0). All components of each reaction, except for Ero1α, were freshly mixed in a total volume of 0.5 ml, and the reaction was initiated by the injection of Ero1α into the reaction vessel of the oxygen electrode. Where present, [Ero1α] = 1 μM, [PDI] = 50 μM, [GPx7] = 20 μM, and [GPx8] = 20 μM. The oxygen consumption rate was calculated from the slope of the linear phase of the consumption curve and normalized relative to the rate calculated on the same day in the presence of Ero1α and PDI. Statistical analysis was performed using a two-tailed paired *t* test.

Accession numbers

The atomic coordinates and structure factors of human GPx8 have been deposited in the PDB under accession code 3KIJ.

Supplementary materials related to this article can be found online at doi:10.1016/j.jmb.2010.12.039

Acknowledgements

This work was supported by the Academy of Finland, Sigrid Juselius Foundation, The Finnish Cultural Foundation, Biocenter Oulu, the University of Oulu, the Chinese Ministry of Science and Technology (2011CB910303), and the Chinese Academy of Sciences (KSCX2-YW-R-119).

References

1. Thorpe, C. & Coppock, D. L. (2007). Generating disulfides in multicellular organisms: emerging roles for a new flavoprotein family. *J. Biol. Chem.* **282**, 13929–13933.
2. Gross, E., Sevier, C. S., Heldman, N., Vitu, E., Bentzur, M., Kaiser, C. A. *et al.* (2006). Generating disulfides enzymatically: reaction products and electron acceptors of the endoplasmic reticulum thiol oxidase Ero1p. *Proc. Natl Acad. Sci. USA*, **103**, 299–304.
3. Enyedi, B., Várnai, P. & Geiszt, M. (2010). Redox state of the endoplasmic reticulum is controlled by Ero1L-α and intraluminal calcium. *Antioxid. Redox Signal.* **13**, 721–729.
4. Appenzeller-Herzog, C., Riemer, J., Christensen, B., Sørensen, E. S. & Ellgaard, L. (2008). A novel disulphide switch mechanism in Ero1α balances ER oxidation in human cells. *EMBO J.* **27**, 2977–2987.
5. Baker, K. M., Chakravarthi, S., Langton, K. P., Sheppard, A. M., Lu, H. & Bulleid, N. J. (2008). Low reduction potential of Ero1α regulatory disulphides ensures tight control of substrate oxidation. *EMBO J.* **27**, 2988–2997.
6. Karala, A. R., Lappi, A. K., Saaranen, M. J. & Ruddock, L. W. (2009). Efficient peroxide mediated oxidative refolding of a protein at physiological pH and implications for oxidative folding in the endoplasmic reticulum. *Antioxid. Redox Signal.* **11**, 963–970.
7. Mills, G. C. (1957). Hemoglobin catabolism. Glutathione peroxidase, an erythrocyte enzyme which protects hemoglobin from oxidative breakdown. *J. Biol. Chem.* **229**, 189–197.
8. Toppo, S., Vanin, S., Bosello, V. & Tosatto, S. C. (2008). Evolutionary and structural insights into the multifaceted glutathione peroxidase (GPx) superfamily. *Antioxid. Redox Signal.* **10**, 1501–1514.
9. Toppo, S., Floché, L., Ursini, F., Vanin, S. & Maiorino, M. (2009). Catalytic mechanisms and specificities of glutathione peroxidases: variations of a basic scheme. *Biochim. Biophys. Acta*, **1790**, 1486–1500.
10. Herbette, S., Roeckel-Drevet, P. & Drevet, J. R. (2007). Seleno-independent glutathione peroxidases more than just simple antioxidant scavengers. *FEBS J.* **274**, 2163–2180.
11. Hatahet, F. & Ruddock, L. W. (2009). Protein disulfide isomerase: a critical evaluation of its function in disulfide bond formation. *Antioxid. Redox Signal.* **11**, 2807–2850.
12. Raykhel, I., Alanen, H., Salo, K., Jurvansuu, J., Nguyen, V. D., Latva-Ranta, M. & Ruddock, L. (2007). A molecular specificity code for the three mammalian KDEL receptors. *J. Cell Biol.* **179**, 1193–1204.
13. Utomo, A., Jiang, X., Furuta, S., Yun, J., Levin, D. S., Wang, Y. C. J. *et al.* (2004). Identification of a novel putative non-selenocysteine containing phospholipid hydroperoxide glutathione peroxidase (NPGPx)

essential for alleviating oxidative stress generated from polyunsaturated fatty acids in breast cancer cells. *J. Biol. Chem.* **279**, 43522–43529.
14. Paglia, D. E. & Valentine, W. N. (1967). Studies on the quantitative and qualitative characterization of erythrocyte glutathione peroxidase. *J. Lab. Clin. Med.* **70**, 158–169.
15. Darby, N. J. & Creighton, T. E. (1995). Characterization of the active site cysteine residues of the thioredoxin-like domains of protein disulfide isomerase. *Biochemistry*, **34**, 16770–16780.
16. Linster, C. L. & Van Schaftingen, E. (2007). Vitamin C. Biosynthesis, recycling and degradation in mammals. *FEBS J.* **274**, 1–22.
17. Alanen, H. I., Williamson, R. A., Howard, M. J., Hatahet, F. S., Salo, K. E., Kauppila, A. *et al.* (2006). ERp27, a new non-catalytic endoplasmic reticulum located human PDI-family member, interacts with ERp57. *J. Biol. Chem.* **281**, 33727–33738.
18. Malhotra, J. D., Miao, H., Zhang, K., Wolfson, A., Pennathur, S., Pipe, S. W. & Kaufman, R. J. (2008). Antioxidants reduce endoplasmic reticulum stress and improve protein secretion. *Proc. Natl Acad. Sci. USA*, **105**, 18525–18530.
19. Tavender, T. J., Sheppard, A. M. & Bulleid, N. J. (2008). Peroxiredoxin IV is an endoplasmic reticulum localized enzyme forming oligomeric complexes in human cells. *Biochem. J.* **411**, 191–199.
20. Tavender, T. J. & Bulleid, N. J. (2010). Peroxiredoxin IV protects cells from oxidative stress by removing H_2O_2 produced during disulphide formation. *J. Cell Sci.* **123**, 2672–2679.
21. Zito, E., Melo, E. P., Yang, Y., Wahlander, Å., Neubert, T. A. & Ron, D. (2010). Oxidative protein folding by an endoplasmic reticulum-localized peroxiredoxin. *Mol. Cell*, **40**, 787–797.
22. Tavender, T. J., Springate, J. J. & Bulleid, N. J. (2010). Recycling of peroxiredoxin IV provides a novel pathway for disulphide formation in the endoplasmic reticulum. *EMBO J.* **29**, 4185–4197.
23. Jessop, C. E., Watkins, R. H., Simmons, J. J., Tasab, M. & Bulleid, N. (2009). Protein disulphide isomerase family members show distinct substrate specificity: P5 is targeted to BiP client proteins. *J. Cell Sci.* **122**, 4287–4295.
24. Alanen, H. I., Salo, K. E. H., Pekkala, M., Siekkinen, H. M., Pirneskoski, A. & Ruddock, L. W. (2003). Defining the domain boundaries of the human protein disulphide isomerases. *Antioxid. Redox Signal.* **5**, 367–374.
25. Karala, A. R. & Ruddock, L. W. (2007). Does *S*-methyl methanethiosulfonate trap the thiol-disulphide state of proteins? *Antioxid. Redox Signal.* **9**, 527–531.
26. Nyfeler, B., Michnick, S. W. & Hauri, H. P. (2005). Capturing protein interactions in the secretory pathway of living cells. *Proc. Natl Acad. Sci. USA*, **102**, 6350–6355.
27. Griesbeck, O., Baird, G. S., Campbell, R. E., Zacharias, D. A. & Tsien, R. Y. (2001). Reducing the environmental sensitivity of yellow fluorescent protein. Mechanism and applications. *J. Biol. Chem.* **276**, 29188–29194.
28. Olivari, S., Galli, C., Alanen, H., Ruddock, L. & Molinari, M. (2005). A novel stress-induced EDEM variant regulating ER-associated glycoprotein degradation. *J. Biol. Chem.* **280**, 2424–2428.
29. Lappi, A. K., Lensink, M. F., Alanen, H. I., Salo, K. E., Lobell, M., Juffer, A. H. & Ruddock, L. W. (2004). A conserved arginine plays a role in the catalytic cycle of the protein disulphide isomerases. *J. Mol. Biol.* **335**, 283–295.
30. Karala, A., Psarrakos, P., Ruddock, L. W. & Klappa, P. (2007). Protein disulphide isomerases from *C. elegans* are equally efficient at thiol-disulphide exchange in simple peptide based systems but show differences in their reactivity towards protein substrates. *Antioxid. Redox Signal.* **9**, 1815–1824.
31. Wang, L., Li, S. J., Sidhu, A., Zhu, L., Liang, Y., Freedman, R. B. & Wang, C. C. (2009). Reconstitution of human Ero1-Lα/protein-disulfide isomerase oxidative folding pathway *in vitro*. Position-dependent differences in role between the a and a′ domains of protein-disulfide isomerase. *J. Biol. Chem.* **284**, 199–206.
32. Horecker, B. L. & Kornberg, A. (1948). The extinction coefficients of the reduced band of pyridine nucleotides. *J. Biol. Chem.* **175**, 385–390.
33. Kursula, P. (2004). XDSi: a graphical interface for the data processing program XDS. *J. Appl. Crystallogr.* **37**, 347–348.
34. Schwarzenbacher, R., Godzik, A., Grzechnik, S. K. & Jaroszewski, L. (2004). The importance of alignment accuracy for molecular replacement. *Acta Crystallogr., Sect. D: Biol. Crystallogr.* **60**, *1229–1236.*
35. Emsley, P. & Cowtan, K. (2004). Coot: model-building tools for molecular graphics. *Acta Crystallogr., Sect. D: Biol. Crystallogr.* **60**, *2126–2132.*
36. Murshudov, A., Vagin, A. & Dodson, E. J. (1997). Refinement of macromolecular structures by the maximum-likelihood method. *Acta Crystallogr., Sect. D: Biol. Crystallogr.* **53**, *240–255.*